CHEMICAL ENGINEERING TRANSACTIONS
VOL. 112, 2024
A publication of AIDIC
The Italian Association of Chemical Engineering
Online at www.cetjournal.it
Guest Editors: Selena Sironi, Laura Capelli

ISBN 979-12-81206-13-7; **ISSN** 2283-9216
DOI: 10.3303/CET24112044

Hybrid Microcrystalline Cellulose-Polyvinylidene Fluoride Membrane for Simultaneous Carbon Dioxide Adsorption and Hydration

Fatin Nasreen Ahmad Rizal Lim, Fauziah Marpani*, Muhammad Akmal Afhammuddin Shamsul, Nur Hidayati Othman, Syazana Mohamad Pauzi, Nik Raikhan Nik Him, Norazah Abd Rahman

School of Chemical Engineering, College of Engineering, Universiti Teknologi MARA, 40450 Shah Alam, Selangor, Malaysia
fauziah176@uitm.edu.my

The alarming high atmospheric carbon dioxide (CO_2) concentrations necessitate the development of effective, low-energy, and eco-friendly CO_2 capture technologies. Polymeric membrane reactors are promising for gas separation due to their ease of fabrication and low energy requirements. However, they often suffer from low mechanical strength, thermal stability, permeability, and selectivity. Mixed matrix membranes (MMMs), which combine polymer matrices with inorganic or organic fillers, address these issues. In this study, MMM was fabricated by incorporating microcrystalline cellulose (MCC) with the polyvinylidene fluoride (PVDF) using non-solvent induced phase separation (NIPS) method. Scanning electron microscopy (SEM) revealed that the membranes have elongated finger-like pores and increases in size with higher MCC content. MMM3 (contain 5.0 wt.% MCC) had the highest porosity and mean pore radius of 55.74 % and 19.05 nm respectively. FTIR and XRD confirmed amorphous structure, and also showing the presence of the MCC and PVDF functional groups. MMMs are more hydrophilic than the pristine membrane, with the lowest water contact angle (84.23°) and high water flux (103.61 ± 8.06 $Lm^{-2}h^{-1}$) is observed in MMM3. The tensile strength of MMMs increased, whilst the elongation-at-break decreased with more MCC. The char yield was the lowest (72.1 %) in MMM3, showing good thermal properties. CO_2 hydrations were measured using titration. All the MMMs showed improved CO_2 hydration performance compared to pristine PVDF. This research demonstrates that adding MCC to PVDF membranes improves hydrophilicity and CO_2 affinity, presenting a sustainable, and low-energy solution for CO_2 capture and reduction.

1. Introduction

The carbon dioxide (CO_2) level in the atmosphere has reached an alarming level. This increase in CO_2, primarily due to uncontrolled human activities, has led to a significant rise in global temperatures. Consequently, we are witnessing a series of drastic events, such as extreme weather patterns and natural disasters. Hence, the mitigation of the greenhouse gas emissions is highly required, and the invention of minimal energy, high efficiency, environmentally benign, and sustainable CO_2 capture and transformation systems are needed. The biocatalytic route is interesting for converting the CO_2 into chemicals because biocatalysts were reported to have excellent selectivity, high specificity, can operate in mild operating conditions, and offer lower input energy than the chemical route. One of the biocatalytic approaches reported was the utilization of the formate dehydrogenase (FDH), formaldehyde dehydrogenase ($F_{ald}DH$), alcohol dehydrogenase (ADH) enzymes, and the reduced nicotinamide adenine dinucleotide (NADH) to transform the CO_2 into methanol (CH_3OH). In this approach, high energy was unnecessary, however, the poor dissolution of CO_2 in water solution and the low stability of the enzymes posed hurdles to the reaction in order to obtain high productivity. Theoretically, higher solubility of CO_2 shall lead to higher CO_2 substrates in the reaction solution, and this could enhance the CO_2 and enzymes interaction, hence raising the overall catalytic efficiency. The hydration rate of CO_2 in water (CO_2 (g) + H_2O (l) ↔ H_2CO_3 (aq)) was reported to be relatively slow (Rasouli, Iliuta, Bougie, Garnier, & Iliuta, 2021).

Paper Received: 29 May 2024; Revised: 18 June 2024; Accepted: 19 August2024
Please cite this article as: Ahmad Rizal Lim F.N., Marpani F., Shamsul M.A.A., Othman N.H., Mohamad Pauzi S., Nik Him N.R., Abd Rahman N., 2024, Hybrid Microcrystalline Cellulose-Polyvinylidene Fluoride Membrane for Simultaneous Carbon Dioxide Adsorption and Hydration, Chemical Engineering Transactions, 112, 259-264 DOI:10.3303/CET24112044

When CO_2 dissolves in water, it shall lead to the formation carbonic acid (H_2CO_3). After that, the H_2CO_3 would dissociate into hydrogen ion (H^+) and bicarbonate ion (HCO_3^-). The HCO_3^- could also further dissociate into H^+ and carbonate ions (CO_3^{2-}). All of the reactions are reversible, hence, causing the easy reformation and escape of CO_2 from the reaction medium, therefore limits the quantity of CO_2 available for reaction (Sinehbaghizadeh, Saptoro, & Mohammadi, 2022). Normally, to improve the dissolvement of CO_2 in water, the application of higher pressure or lower temperature would be suggested, however, this phenomena could easily affect the catalytic activity of the enzymes (Yuan, Shen, & Salmon, 2023). Other than that, the most effective method reported was by employing carbonic anhydrase (CA) enzyme to catalyze the hydration of CO_2. To maintain its stability and facilitate its reusability for multiple cycles, Rasouli et al. (Rasouli et al., 2021) had covalently immobilized CA by utilizing glutaraldehyde (GA) on amine functionalized surface of flat-sheet polypropylene (PP) membrane. The biocatalytic membrane system had achieved a CO_2 permeance approximately around 0.29×10^{-3} mol m^{-2} s^{-1}, and storage stability for about 40 days. Recently, it was reported that the introduction of amine-rich compound could facilitate the transformation of CO_2 to HCO_3^- with the presence of water. Pu et al. (Pu et al., 2024) had produced an amine-rich metal organic framework (MOF) membrane, which is by blending polyethylenimine (PEI) polymers with NUS-8 to enhance the CO_2 capture capability. It was highlighted that by increasing higher PEI content, both of the CO_2 permeability and selectivity of the PEI/NUS membrane would increase, and the results had also proved that the presence of water was necessary for aiding the CO_2 transfer.

The application of membrane contactors in aiding the CO_2 capture and conversion are compelling because they possess large surface area, easy to fabricate, able to facilitate the contact between CO_2 gas and the aqueous solution. They are also excellent supports for enzyme immobilization (Liao et al., 2023). The application of nanocellulose (NC)-based polymeric membranes could provide high surface area and hydroxyl groups, which could act as cross-linking agents and adsorption sites for the CO_2 gas (Zhang et al., 2024). Not only that, the hydroxyl groups in NC could form hydrogen bonds with the CO_2 molecules, and facilitating its hydration. Although CO_2 is a non-polar molecule, due to the carbon-oxygen double bonds (C=O), it can interact with the polar hydroxyl groups (-OH), hence, facilitating the solubilization of CO_2 in water. The abundance hydroxyl groups could also increase the amount of water molecules available to react with CO_2. There are several types of NC that have been studied for CO_2 separations and improving the water permeability of polymeric membranes. For instance, cellulose nanocrystals (CNC), cellulose nanofibrils (CNF), and bacterial cellulose (BC). Jahan et al. (Jahan, Niazi, Hägg, & Gregersen, 2018) had established a nanocomposite membrane by combining CNC with polyvinyl alcohol (PVA) membrane for separation of CO_2 and CH_4 gases. Due to the ability of CNC to exhibit high degree of swelling when exposed to a humid environment, the composite membrane with 1 % CNC was able to aid the CO_2 transport, and improved the CO_2 permeability and CO_2/CH_4 selectivity of the PVA membrane. Nazri et al. (Nazri, AMMMad, & Hussin, 2021) had blended microcrystalline cellulose (MCC) with polyethersulfone (PES) membrane, and it had provided approximately 20 times higher pure water flux then the pristine PES membrane, indicating improved hydrophilicity properties. In this work, MMMs were fabricated by incorporating MCC and PVDF to study its performance towards CO_2 adsorption and hydration. The amount of MCC content in the MMM was varied to study its effects on the morphology, surface chemistry, crystalline structure, porosity, hydrophilicity, thermal stability, and mechanical properties. Lastly, the performance of the MMMs towards water permeation test and CO_2 hydration were evaluated.

2. Experimental

2.1 Materials

Microcrystalline cellulose (MCC) and Dimethylformamide (DMF) were from Sigma Aldrich, Germany and polyvinylidene fluoride (PVDF) resins (Kynar 760) from Arkema. Pure CO_2 gas (>99%) supplied by Linde, Malaysia.

2.2 Fabrication of hybrid membrane

For 100 g of casting solution for MMM1, 79.5 g of DMF and 0.5 g of MCC powder were mixed and stirred at 80°C until a homogeneous MCC solution was achieved, and then immersed in an ultrasonicator at 60°C for 1 hour. Same procedures were repeated for the other MMMs. A casting solution with 20.0 wt.% PVDF pellets, combined with MCC solution, and stirred at 65°C until homogeneous and degassed in an ultrasonic bath at 60°C for 1 hour. The dope was casted on a glass plate and then immersed in water bath. The membrane sheets were washed with tap water, soaked in a distilled water coagulation bath for a day, and stored in fresh distilled water before use. Table 1 summarized the denotion of MMMs with respect to its composition.

Table 1: Composition of the casting solutions used to fabricate membrane in this work.

Composition (wt%)	Pristine	MMM1	MMM2	MMM3
PVDF	20.0	20.0	020	20.0
MCC	-	0.5	0.5	2.0
DMF	80.0	79.5	79.5	78.0

2.3 Characterization

The MMMs morphologies were analysed using SEM (S-3400 N, Hitachi, Tokyo, Japan). The presence of functional groups and chemical bonds in the membranes were determined by using FTIR scanned in the frequency range of 500 – 4000 cm^{-1}. The membrane was immersed into ultrapure water for 24 h and the weight of the wet membranes were taken. The membrane was then dried to obtain the mass of dried membrane. The porosity of the membrane (ε_m) and mean pore radius (r_m) were calculated by using Eqn. (4) and (5) respectively (Junaidi et al., 2020). The water contact angle (WCA) was measured using goniometer (VCA-3000 s, AST Products Inc., Massachusetts, USA). The mechanical properties of the membranes were determined by using a H50KT-S mechanical tester based on ASTM D882 standard method. The thermal stability was carried out in a TGA (Mettler Toledo) under nitrogen (N_2) atmosphere and heated up to 800 °C at a heating rate of 10 °C min^{-1}. X-ray diffraction (Rigaku Ultima III, Japan) with a scan range of 2θ = 4 - 90°, and rate of 6° min^{-1}, with Cu-K∝ radiation, a nickel filter, a wavelength of 0.154 nm was employed.

2.4 Water permeability and hydration study

The water permeation test was conducted via a 50 mL stirred cell (Amicon 8050, Millipore, USA) with an effective membrane surface area of 13.4 cm^2. A pressure of 4 bar was supplied by N_2. The permeate was collected calculated by using Eqn. (6). The hydration of CO_2 was measured by acid-base titration method. Pure CO_2 was bubbled in a 20 mL of 0.1 M phosphate buffer (pH 7.0) for 10 minutes, then filtrated via MMM-equipped stirred cell. The NaOH solution was titrated into the permeate collected until light pink color appeared. The volume of NaOH was recorded and the amount of CO_2 hydrated (M_2) was calculated using Eqn. (7).

Table 2: List of equations.

Eqn. no.	Eqn.	Description/ units	Variables
4	$\varepsilon_m = \frac{(w_1-w_2)/\rho_w \times 100\ \%}{(w_1-w_2)/\rho_w+(w_2/\rho_{PVDF})}$	Membrane porosity (%)	w_1 = wet membrane weight (g), w_2 = dry membrane (g), ρ_w = water density ($g\ cm^{-3}$), ρ_{PVDF} = PVDF density ($g\ cm^{-3}$)
5	$r_m = \sqrt{\frac{(2.95-1.75\varepsilon_m)\times 8l\eta Q}{\varepsilon_m \times A \times \Delta P}}$	Mean pore radius (nm)	η = water viscosity (8.90×10^{-4} Pa.s), Q = permeate (in $m^3\ s^{-1}$), l = membrane thickness (m), ε_m = membrane porosity, A = membrane (m^2), ΔP = operating pressure (1.00×10^5 Pa)
6	$Q_i = \frac{V}{A \times t}$	Permeate flux, ($L\ m^{-2}\ h^{-1}$)	V = volume of permeate collected, A = membrane area (m^2), t = filtration time (h)
7	$M_2 = (M_1V_1)/V_2$	Dilution (M)	M_1 = [NaOH] (0.1 M), V_1 = NaOH volume, M_2 = [H_2CO_3] in the solution, V_2 = H_2CO_3 volume (20 mL)

3. Results and discussion

The MMMs have developed an asymmetric structure and showed uniform pores distribution (Figure 1). The possession of interactive hydroxyl groups by the MCC could form hydrogen bonding with the polymer matrix, hence influencing the final morphology and porosity of the membranes. The cross-sectional image shows wide elongated finger-like pores as the MCC content increases (Figure 1). The MMM1 (Figure 1f) showed the most uniform finger-like structures, but MMM2 (Figure 1g) and MMM3 (Figure 1h) possessed more macrovoids. MCC can act as physical spacer when it interacts with a polymer matrix by occupying the space within the polymer matrix, hence become the physical barriers that would prevent the polymer chains from aligning closely, leading to the formation of void spaces around the MCC particles (Hosakun, Halász, Horváth, Csóka, & Djoković, 2017). Well-dispersed MCC is able to act as the nucleation sites for the pore formation, whereas the unevenly dispersed MCC could lead to agglomeration and larger, but less uniform pores, which had shown by MMM3 (Figure 1h), where the membrane pores are not as uniform as MMM1 (Figure 1f). The fabricated pristine PVDF membrane had showed an absorption peak at 1179 cm^{-1}, which assigned to the C-F group (Xu, Lin, Chew, Malde, & Wang, 2019) (Figure 2a). The C-H bending for the pristine PVDF membranes were shown at the peak of 874, and 762 cm^{-1} (Dong et al., 2022). The broad absorption band from 3400 cm^{-1} to 3200 cm^{-1} represents the stretching of OH groups, which indicates the existence of MCC on the surface of all the hybrid MCC/PVDF membranes (Nazri

et al., 2021; Valdebenito et al., 2018). Strong C-O stretching were also detected at the peak of 1067 cm^{-1} (Bai, Wang, Zhou, & Zhang, 2012). A visible peak at 20.4° was noticed for all of the samples (Figure 2b), which indicate the (2,0,0) plane of PVDF and can be confirmed by JCPDS 42-1649. From the XRD spectra obtained and the absence of obvious diffraction peaks, the MMM consist of CNC amorphous structure, which can be observed at 2θ = 18° (Bai et al., 2012).

MMM3 shows the highest porosity (56%) followed by MMM2 (44%). The addition of MCC proved porosity enhancement, where all of the MMMs show higher porosity than the pristine membrane (Figure 2c). The membrane pore size could be affected by the penetration velocity of water-solvent during the phase transformation (Junaidi et al., 2020), while MCC restrict the mobility of the polymer chains during solidification process, thus promoting the formation of a more open, and porous structure (Sunder, Fong, & Bustam, 2022). MMM3 mean pore radius value is about 19 nm, whilst the pristine membrane is 3.9 nm. Higher porosity allows more water molecules to permeate and diffuse through the membrane promoting the membrane's hydrophilicity and permeability (Bai et al., 2012). MMM3 shows lower WCA than MMM2 implying that MMM3 is more hydrophilic than MMM2. Higher MCC contributes to more OH groups on the surface of membrane, hence attracting water to fill up the air gaps on the membrane surface, thus promoting membrane wetting. MMM1 shows the highest elongation-at-break and tensile strength, which are 29.30 ± 0.28 %, and 18.20 ± 2.97 MPa respectively (Figure 2e). Hydroxyl groups promote hydrogen bonding within the matrix and provides additional cohesions between components, which may enhance its mechanical strength. The TGA curve shows the weight losses between the temperatures of 300 – 500 °C indicating that the organic molecules had started to degrade (Figure 5d). The decomposition temperature of MMM is about 326 °C, which is significantly different from that of pristine (470 °C). The char yield for the MMMs can be summarized in the order of pristine (81.1 %) > MMM1 (78.1 %) > MMM2 (75.5 %) > MMM3 (72.1 %). This proved that the introduction of MCC improved the thermal properties of the MMMs.

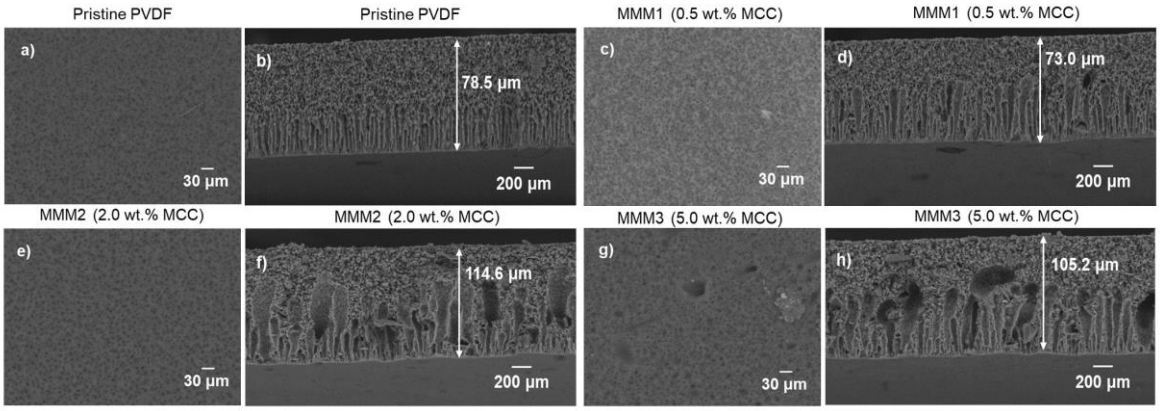

Figure 1: SEM images showing the top surface of (a) the pristine PVDF membrane, (c) MMM1, (e) MMM2, and (g) MMM3, as well as the cross-section views of (b) the pristine PVDF membrane, (d) MMM1, (f) MMM2, and (h) MMM3 respectively.

The pristine PVDF showed the lowest PWF of 3.82 ± 0.81 L m^{-2} h^{-1} due to the smallest pore size, and it was also less hydrophilic compared to MMMs. The highest PWF was exhibited by MMM3, which was at 103.61 ± 8.06 L m^{-2} h^{-1}. PWF of the hybrid membranes increase with the increment of MCC content (Figure 3a). The presence of the OH groups from MCC attracted water molecules more easily to the membrane surface which lead to the increase of water permeability.

The MMM fabricated in this study will be further applied in enzymatic membrane reactor in an effort to reduce CO_2. It is known that CO_2 is thermodynamically stable molecule, and it has low solubility and hydration in water. The hydrated CO_2 species can be easily uptake by FDH (EC1.2.1.46) to be further reduced into formic acid (CHOOH) (Ji, Su, Wang, Ma, & Zhang, 2015). Earlier, it was hypothesized that the abundant hydroxyl groups provided by MCC could facilitate the hydration of the adsorbed CO_2 to H_2CO_3 through Lewis acid-base interactions. The HCO_3^- produced shall bind to the metal (molybdenum or tungsten) cofactor (which located at the active site of FDH), making it more electrophilic and prepares it to undergo nucleophilic attack. NADH donate a hydride ion (H^-), which would attack the carbon atom of the activated CO_2 and forms an intermediate, $HCOO^-$ (Marpani, Pinelo, & Meyer, 2017). A proton (H^+) is transferred to the oxygen atom of the intermediate and leading to the formation of formic acid (HCOOH). Figure 3b shows CO_2 hydration rate for all the membranes. The highest CO_2 hydration is recorded at 4.93 mM s^{-1} when MMM3 is used. This marked more than 40 % improvement of

CO_2 hydration in comparison with pristine PVDF membrane at 2.25 mM s^{-1} (Figure 3b). Abundance of hydroxyl groups in MCC particularly on the membrane surface, create a network of hydrogen bonds with water molecules, leading to improved water retention and interactions (Zhang et al., 2024). In water-catalyzed CO_2 hydration, water oxygen attacks the CO_2 carbon while a water hydrogen atom transfers to CO_2 oxygen via a chain of water molecules, forming a ring-shaped transition state. Increasing the amount of water molecules in the chain, mediated by the hydrophilic membrane surface, reduce the activation energy required for CO_2 hydration (Nguyen, Raspoet, Vanquickenborne, & Van Duijnen, 1997).

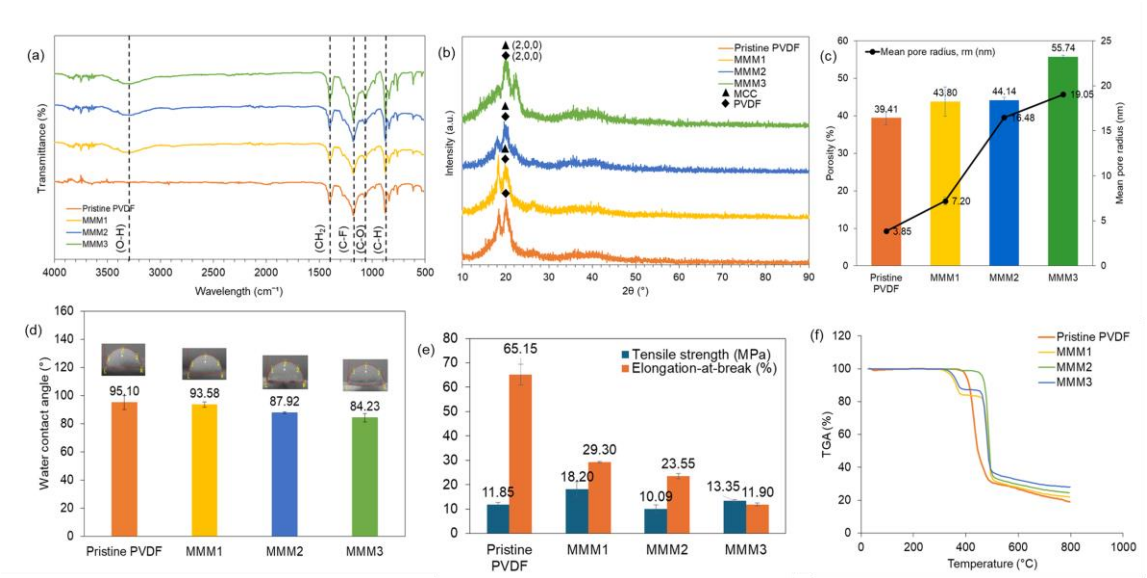

Figure 2: (a) FTIR spectra, (b) XRD patterns, (c) Porosity and mean pore radius, (d) Average WCA, (e) Average tensile strength and elongation-at-break, and (f) TGA curves of the fabricated flat-sheet pristine PVDF membrane, and MMMs in this study.

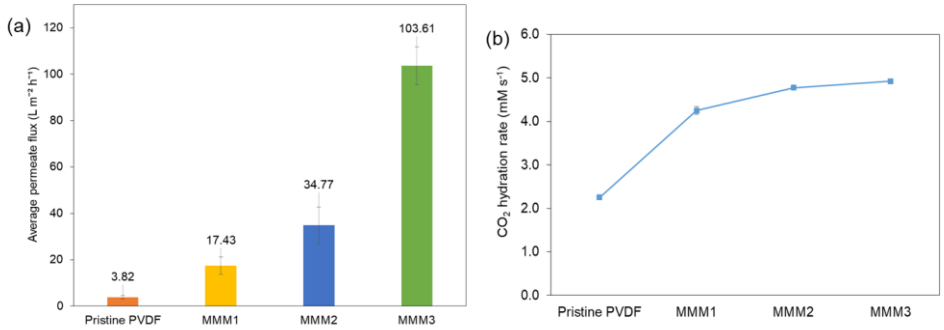

Figure 3: (a) Permeate flux profile, (b) CO_2 hydration rate of the fabricated pristine PVDF, and MMMs respectively.

4. Conclusion

This work focuses on development of MCC and PVDF hybrid membrane to improve the hydration of CO_2 in aqueous solution. The MMMs showed promising physicochemical properties and performance than the pristine PVDF membrane. The highest porosity and pore size were presented by MMM3. FTIR and XRD confirmed the presence of MCC and PVDF, indicating successful blending of the materials. MMMs were more hydrophilic than the pristine membrane, with tensile strength increased while elongation-at-break decreased with more MCC, with better thermal stability. The CO_2 hydration rate of recorded 4.93 mM s^{-1}, highlighting MCC incorporated PVDF membranes improves hydrophilicity and CO_2 affinity, presenting a sustainable, low energy solution for CO_2 capture.

Acknowledgments

This research was funded by the Malaysia Ministry of Higher Education (MOHE) under the Fundamental Research Grant Scheme (FRGS) funding (FRGS/1/2019/TK02/UITM/03/5).

References

Bai, H., Wang, X., Zhou, Y., & Zhang, L. (2012). Preparation and characterization of poly(vinylidene fluoride) composite membranes blended with nano-crystalline cellulose. *Progress in Natural Science: Materials International*, *22*(3), 250–257. https://doi.org/10.1016/j.pnsc.2012.04.011

Dong, S., Huang, W., Li, X., Wang, X., Yan, B., Zhang, Z., & Zhong, J. (2022). Synthesis of dual-functionalized APTES-Bentonite/PVDF mixed-matrix membranes for the efficient separation of CO2/CH4 and CO2/N2. *Materials Today Communications*, *31*(March), 103431. https://doi.org/10.1016/j.mtcomm.2022.103431

Hosakun, Y., Halász, K., Horváth, M., Csóka, L., & Djoković, V. (2017). ATR-FTIR study of the interaction of CO2 with bacterial cellulose-based membranes. *Chemical Engineering Journal*, *324*, 83–92. https://doi.org/10.1016/j.cej.2017.05.029

Jahan, Z., Niazi, M. B. K., Hägg, M. B., & Gregersen, Ø. W. (2018). Cellulose nanocrystal/PVA nanocomposite membranes for CO2/CH4 separation at high pressure. *Journal of Membrane Science*, *554*(October 2017), 275–281. https://doi.org/10.1016/j.memsci.2018.02.061

Ji, X., Su, Z., Wang, P., Ma, G., & Zhang, S. (2015). Tethering of nicotinamide adenine dinucleotide inside hollow nanofibers for high-yield synthesis of methanol from carbon dioxide catalyzed by coencapsulated multienzymes. *ACS Nano*, *9*(4), 4600–4610.

Junaidi, N. F. D., OtMMMan, N. H., Shahruddin, M. Z., Alias, N. H., Marpani, F., Lau, W. J., & Ismail, A. F. (2020). Fabrication and characterization of graphene oxide–polyethersulfone (GO–PES) composite flat sheet and hollow fiber membranes for oil–water separation. *Journal of Chemical Technology & Biotechnology*, *95*(5), 1308–1320. https://doi.org/10.1002/jctb.6366

Liao, Q., Guo, M., Mao, M., Gao, R., Meng, Z., Fan, X., & Liu, W. (2023). Construction and optimization of a photo−enzyme coupled system for sustainable CO2 conversion to methanol. *Process Biochemistry*, *129*(December 2022), 44–55. https://doi.org/10.1016/j.procbio.2023.03.011

Marpani, F., Pinelo, M., & Meyer, A. S. (2017). Enzymatic conversion of CO2 to CH3OH via reverse dehydrogenase cascade biocatalysis: Quantitative comparison of efficiencies of immobilized enzyme systems. *Biochemical Engineering Journal*, *127*, 217–228. https://doi.org/10.1016/j.bej.2017.08.011

Nazri, A. I., AMMMad, A. L., & Hussin, M. H. (2021). Microcrystalline cellulose-blended polyethersulfone membranes for enhanced water permeability and humic acid removal. *Membranes*, *11*(9). https://doi.org/10.3390/membranes11090660

Nguyen, M. T., Raspoet, G., Vanquickenborne, L. G., & Van Duijnen, P. T. (1997). How many water molecules are actively involved in the neutral hydration of carbon dioxide? *Journal of Physical Chemistry A*, *101*(40), 7379–7388. https://doi.org/10.1021/jp9701045

Pu, Y., He, G., Zhao, M., Yang, Z., Li, H., Ren, Y., … Jiang, Z. (2024). Polymer-functionalized metal-organic framework nanosheet membranes for efficient CO2 capture. *Journal of Membrane Science*, *707*(June). https://doi.org/10.1016/j.memsci.2024.123018

Rasouli, H., Iliuta, I., Bougie, F., Garnier, A., & Iliuta, M. C. (2021). Enzyme-immobilized flat-sheet membrane contactor for green carbon capture. *Chemical Engineering Journal*, *421*, 129587. https://doi.org/10.1016/j.cej.2021.129587

Sinehbaghizadeh, S., Saptoro, A., & Mohammadi, A. H. (2022). CO2 hydrate properties and applications: A state of the art. *Progress in Energy and Combustion Science*, *93*(July 2021), 101026. https://doi.org/10.1016/j.pecs.2022.101026

Sunder, N., Fong, Y. Y., & Bustam, M. A. (2022). Investigation on the effects of air gap distance on the formation of cellulose triacetate hollow fiber membrane for CO2 and CH4 gases permeation. *Materials Today: Proceedings*, (xxxx), 2–6. https://doi.org/10.1016/j.matpr.2022.02.280

Valdebenito, F., García, R., Cruces, K., Ciudad, G., Chinga-Carrasco, G., & Habibi, Y. (2018). CO2 Adsorption of Surface-Modified Cellulose Nanofibril Films Derived from Agricultural Wastes. *ACS Sustainable Chemistry and Engineering*, *6*(10), 12603–12612. https://doi.org/10.1021/acssuschemeng.8b00771

Xu, Y., Lin, Y., Chew, N. G. P., Malde, C., & Wang, R. (2019). Biocatalytic PVDF composite hollow fiber membranes for CO2 removal in gas-liquid membrane contactor. *Journal of Membrane Science*, *572*(August 2018), 532–544. https://doi.org/10.1016/j.memsci.2018.11.043

Yuan, Y., Shen, J., & Salmon, S. (2023). Developing Enzyme Immobilization with Fibrous Membranes: Longevity and Characterization Considerations. *Membranes*, *13*(5). https://doi.org/10.3390/membranes13050532

Zhang, M., Xu, T., Zhao, Q., Liu, K., Liang, D., & Si, C. (2024). Cellulose-based materials for carbon capture and conversion. *Carbon Capture Science & Technology*, *10*(November 2023), 100157. https://doi.org/10.1016/j.ccst.2023.100157